European **J**ournal of **Chem**istry

Check for updates

Synthesis, molecular docking, and biological evaluation of methyl-5-(hydroxyimino)-3-(aryl-substituted)hexanoate derivatives

Parashuram Gudimani [iD] 1, Samundeeswari Lokesh Shastri [iD] 1, Varsha Pawar [iD] 1, Nagashree Uday Hebbar [iD] 1, Lokesh Anand Shastri [iD] 1,*, Shrinivas Joshi [iD] 2, Shyam Kumar Vootla [iD] 3, Sheela Khanapure [iD] 3 and Vinay Sunagar [iD] 4

1 Department of Chemistry, Karnatak University, Dharwad 580003, Karnataka, India
2 Novel Drug Design and Discovery Laboratory, Department of Pharmaceutical Chemistry, Soniya Education Trusts College of Pharmacy, SangolliRayanna Nagar, Dharwad 580002, Karnataka, India
3 Department of Biotechnology and Microbiology, Karnatak University, Dharwad 580003, Karnataka, India
4 Department of Chemistry, Govindram Seksaria Science College, Belagavi 590006, Karnataka, India

* Corresponding author at: Department of Chemistry, Karnatak University, Dharwad 580003, Karnataka, India.
 e-mail: drlashastri@kud.ac.in (L.A. Shastri).

RESEARCH ARTICLE

KEYWORDS

ABSTRACT

Beta-aryl keto hexanoic acids (5a-l) were synthesized efficiently, followed by esterification that afforded beta-aryl keto methylhexanoates (6a-l). The chemo-selective ketoxime beta-aryl methyl hexanoates (7a-l) were isolated in good yields. Spectroscopic methods were used to characterize the obtained moieties. The antioxidant, anti-inflammatory, and antibacterial properties of the effectively synthesized compounds 7a-l were also investigated. The anti-inflammatory activity of the compounds 7c, 7f, 7i, and 7l was excellent, with a low IC$_{50}$ value at micromolar concentration, which was much better than the reference diclofenac. All synthesized compounds 7a-l were assessed for their *in vitro* antibacterial activity against *S. aureus, B. subtilis* and *E. coli.* Most of the compounds exhibited promising activity against Gram-positive bacterial strain, compound 7i showed excellent activity compared to standard streptomycin and in the case of *E. coli,* compounds 7b, 7c, 7j, 7k and 7l have shown moderate activity. Further, the cytotoxic activities of the compounds were assessed against lung cancer cells (A549) by using MTT assay. The possible interaction mechanism of the molecules 7c and 7g with Gram-negative strain *E. coli* DNA gyrase B in complex with PDB ID: 4DUH was studied.

1. Introduction

Synthetic organic moieties have gained popularity in recent years, particularly in material chemistry, and biological applications [1]. Small organic moieties with functional bunch activation can lead to the formation of novel chemical bonds, which have shown higher pharmacological action. For example, oxime and its derivatives are a common class of organic fragments that find use in both synthetic and medicinal chemistry [2]. Oxime derivatives increased their organic, inorganic, industrial, analytical, and biochemistry demands. Oximes are a critical intermediate in a variety of domains; including coordination, polymer, and materials chemistry, as well as the chemical trade industry [3,4]. They have attracted a lot of attention because of their coordinating ability, and oxime products are preferred for refinement, identification, and protection of carbonyl moieties, especially for α-activation and are very helpful in synthetic organic chemistry [5,6].

Reconstruction of functional groups is an important step in synthetic organic chemistry, and oxime is an important intermediate in the synthesis of amides, amines, and hydroxylamine-o-ether, as well as in the Beckmann reaction. As a result, chemists are particularly interested in making oximes. Oximes of carbonyl group compounds are significant not only for shielding, refining, and structural identification but also for converting a wide range of functional groups [7]. Oximes of carbonyl group compounds are significant not only for shielding, refining, and structural identification but also for converting a wide range of functional groups [8]. When an oxime is made with a keto-carbonyl group and the introduction of oxime group in a molecule, its biological activity increases considerably [9,10].

The scaffolds of hydroxamic acids are exhibiting antibacterial, antifungal, anti-inflammatory, antiviral, antioxidant, fungicidal, herbicidal, and anticancer properties [11-18], and are complex former [19,20].
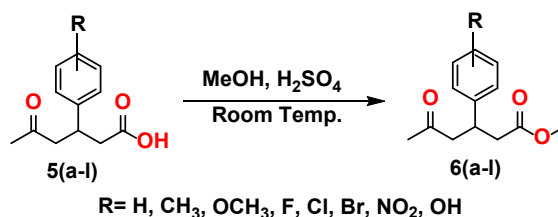
Scheme 1. Synthesis of methyl 5-oxo-3-(aryl-substituted)hexanoate derivatives **6a-l**.
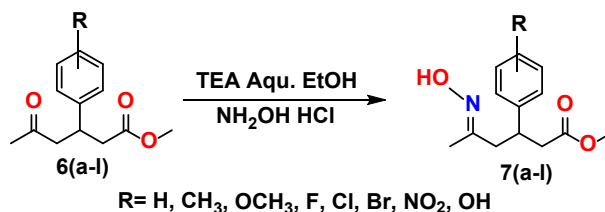
Scheme 2. Synthesis of methyl 5-(hydroxyimino)-3-(aryl-substituted)hexanoate derivatives **7a-l**.

Furthermore, in the proximity of the hydroxamic acid group, there is a decreased risk of poisoning or toxicity [21]. Hydroxamic acid research is ongoing [22], with the goal of improving the precursor properties. Whereas, oximes having aromatic, hetero-aromatic, and alip-hatic scaffolds exhibit excellent anti-inflammatory activity [23-25].

Bacterial and fungal infections are threatening human health, for this reason, there is a strong need to create anti-microbial medications that are effective against a wide range of microbes for lengthy periods [26,27]. Antibiotics are used to treat the microorganism pandemic, but most of them have adverse effects and are used inadvertly, to which the immune system reacts [28]. Moreover, the infection syndrome spreads quickly when bacteria develop resistance to antibiotics. Additionally, there is a provision for an advanced grade of antimicrobial helpers that differs from the present ones and overcomes all above-mentioned issues. Antibacterial and antifungal scaffolds are being researched extensively through-out the world [29].

Continuation of our research on the pyran scaffold [30] and ketohexanoic acid [31], the current study focuses on the efficient, practical and cost-effective synthesis of oxime deriva-tives and their biological activity. The major purpose is to develop novel compounds and testing their anti-inflammatory, antioxidant, antibacterial, and cytotoxic capabilities.

2. Experimental

2.1. Materials and methods

All reactions were carried out with analytical grade chemicals, 5-oxo-3-(aryl-substituted)hexanoic acids (**5a-l**) were synthesised using a sequential process described in elsver [31] and substituted-4*H*-pyran-3-carboxylate was produced using a procedure described in the literature [30]. The melting points were determined using open capillary technique. The Fourier Transform infrared (FT-IR) spectra were recorded using a PE spectrum (IR version 10.6.1) and Nuclear Magnetic Resonance (NMR) data was recorded using Jeol 400 MHz spectrometer. The chemical shifts were reported in a parts per million (ppm) scale using deuterated dimethyl sulphoxide (DMSO-d_6) and deuterated chloroform (CDCl$_3$) as solvents and tetramethylsilane (TMS) as an internal standard. Mass spectra were recorded using an Agilent single Quartz LC-MS spectrum.

2.2. Synthesis of entitled compounds

2.2.1. General synthetic route for the preparation of methyl-5-oxo-3-(aryl-substituted)hexanoate derivatives (6a-l)

At room temperature, 5-oxo-3-(ary*l*-substituted)hexanoic acids (**5a-l**) (1 mmol) were treated with methanol (5 mL) in the presence of catalytical quantity of sulphuric acid (2 drops) (Scheme 1) and stirred for 2-3 hrs. The progress and completion of the reaction was monitored and confirmed by TLC. The excess methanol was removed by rota evaporator. After concentration, the reaction mixture was poured into ice cold water, obtained solid was filtered and washed with cold ethanol to procure the pure compound.

2.2.2. Synthesis of methyl-5-(hydroxyimino)-3-(aryl-substituted)hexanoate derivatives (7a-l)

The targeted moieties (**7a-l**) were synthesized in the pure form without column chromatography, in the presence of catalytic amount of base (2-3 drops) triethyl amine (TEA) by treating compounds **6a-l** (1 mmol) with hydroxylamine hydrochloride (1 mmol) at room temperature, using 5 mL of ethanol as solvent (Scheme 2). The reaction was monitored by TLC, when completion of the reaction was confirmed, after 4-5 hrs, the mixture was poured into crushed ice, the separated solid was filtered and washed with water and cold ethanol.

Methyl-5-(hydroxyimino)-3-phenylhexanoate (**7a**): Color: White solid. Yield: 90%. M.p.: 70-72 °C. FT-IR (KBr, ν, cm^{-1}): 3222 (NH) and 1728 (C=O). ^{1}H NMR (400 MHz, CDCl$_3$, δ, ppm): 1.82 (s, 3H, CH$_3$), 2.44-2.55 (m, 2H, CH$_2$), 2.56-2.70 (m, 2H, CH$_2$), 3.40-3.48 (m, 1H, CH), 3.55 (s, 3H, OCH$_3$), 7.18 (d, *J* = 7.9 Hz, 2H, Ar-H), 7.28 (t, *J* = 7.6 Hz, 3H, Ar-H), 8.68 (s, 1H, OH). ^{13}C NMR (100 MHz, CDCl$_3$, δ, ppm): 13.75, 39.31, 40.59, 42.40, 51.72, 126.95, 127.33, 128.72, 143.04, 156.64, 172.62. LC-MS (*m/z*): 235.

Methyl-5-(hydroxyimino)-3-(p-tolyl)hexanoate (**7b**): Color: White solid. Yield: 84%. M.p.: 88-90 °C. FT-IR (KBr, ν, cm^{-1}): 3288 (NH) and 1707 (C=O). ^{1}H NMR (400 MHz, DMSO-d_6, δ, ppm): 1.90 (s, 3H, CH$_3$), 2.15 (s, 3H, Ar-C*H*$_3$), 2.55 (m, 2H, CH$_2$), 2.65 (m, 2H, CH$_2$), 3.49 (m, 1H, CH), 3.56 (3H, s, OCH$_3$), 7.40 (d, *J* = 8.0, Hz, 2H, Ar-H), 8.17 (d, *J* = 8.0, Hz, 2H, Ar-H) 9.20 (s, 1H, OH). ^{13}C NMR (100 MHz, DMSO-d_6, δ, ppm): 13.5, 21.8, 27.4, 37.9, 41.8, 51.7, 127.2 129.4 ,140.5,143.7, 158.6 ,172.8. LC-MS (*m/z*): 249.

Methyl-3-(4-chlorophenyl)-5-(hydroxyimino)hexanoate (**7c**): Color: Brown viscous liquid. Yield: 98%. FT-IR (KBr, ν, cm⁻¹): 3265 (NH) and 1727 (C=O). ¹H NMR (400 MHz, DMSO-d_6, δ, ppm): 1.63 (s, 3H, CH₃), 2.32-2.41 (m, 2H, CH₂), 2.55-2.80 (m, 2H, CH₂), 3.44 (s, 3H, OCH₃), 3.89 (q, *J* = 3.1 Hz, 1H, CH), 7.24 (d, *J* = 3.8 Hz, 2H, Ar-H), 7.27 (d, *J* = 8.4 Hz, 2H, Ar-H), 10.31 (s, 1H, OH). ¹³C NMR (100 MHz, DMSO-d_6, δ, ppm): 13.93, 30.61, 38.86, 42.04, 51.74, 128.63, 129.90, 131.47, 142.87, 153.79, 171.75. LC-MS (*m/z*): 269.

Methyl-3-(4-fluorophenyl)-5-(hydroxyimino)hexanoate (**7d**): Color: White solid. Yield: 90%. M.p.: 78-80 °C. FT-IR (KBr, ν, cm⁻¹): 3254 (NH) and 1700 (C=O). ¹H NMR (400 MHz, DMSO-d_6, δ, ppm): 1.62 (s, 3H, CH₃), 2.74-2.27 (m, 4H, CH₂), 3.51 (s, 3H, OCH₃), 3.34, (s, 1H, CH), 7.14-6.94 (d, 2H, Ar-H), 7.33-7.13 (d, 2H, Ar-H), 10.27 (s, 1H, OH). ¹³C NMR (100 MHz, DMSO-d_6, δ, ppm): 13.93, 35.16, 38.61, 42.21, 51.74, 115.52, 129.76, 140.19, 153.86, 162.55, 172.53. LC-MS (*m/z*): 253.

Methyl-5-(hydroxyimino)-3-(4-methoxyphenyl)hexanoate (**7e**): Color: Light yellow. Yield: 80%. M.p.: 76-78 °C. FT-IR (KBr, ν, cm⁻¹): 3244 (NH) and 1723 (C=O). ¹H NMR (400 MHz, DMSO-d_6, δ, ppm): 1.82 (s, 3H, CH₃), 2.40 (m, 2H, CH₂), 2.42 (m, 2H, CH₂), 3.40 (m, 1H, CH), 3.50 (s, 3H, OCH₃), 3.60 (s, 3H, OCH₃), 7.20 (d, *J* = 8.8 Hz, 2H, Ar-H), 7.42 (d, *J* = 8.8 Hz, 2H, Ar-H) 9.70 (s, 1H, OH). ¹³C NMR (100 MHz, DMSO-d_6, δ, ppm): 13.5, 31.9, 37.5, 41.5, 51.2, 54.0, 116.3, 129.7, 145.3, 158.6, 160.8, 172.2. LC-MS (*m/z*): 265.

Methyl-5-(hydroxyimino)-3-(4-hydroxyphenyl)hexanoate (**7f**): Color: Yellow solid. Yield: 80%. M.p.: 72-74 °C. FT-IR (KBr, ν, cm⁻¹): 3245 (NH) and 1715 (C=O). ¹H NMR (400 MHz, DMSO-d_6, δ, ppm): 1.62 (s, 3H, CH₃) 2.68-2.35 (m, 4H, CH₂), 3.38 (m, 1H, CH), 3.52 (d, *J* = 71.7 Hz, 3H, OCH₃), 7.13-8.10 (d, *J* = 77.8 Hz, 4H, Ar-H), 10.27 (s, 1H, OH). ¹³C NMR (100 MHz, DMSO-d_6, δ, ppm): 13.9, 35.2, 38.6, 42.2, 51.7, 115.3, 115.5, 129.8, 129.8, 140.1, 153.9, 160.1, 162.5, 172.4. LC-MS (*m/z*): 251.

Methyl-5-(hydroxyimino)-3-(4-nitrophenyl)hexanoate (**7g**): Color: White solid. Yield: 98%. M.p.: 76-78 °C. FT-IR (KBr, ν, cm⁻¹): 3215 (NH) and 1723 (C=O). ¹H NMR (400 MHz, CDCl₃, δ, ppm): 1.82 (s, 3H, CH₃), 2.47-2.63 (m, 2H, CH₂), 2.73 (dd, *J* = 16.0, 6.1 Hz, 2H, CH₂), 3.57 (s, 3H, OCH₃), 3.64-3.72 (m, 1H, CH), 7.35 (d, *J* = 8.4 Hz, 2H, Ar-H), 8.02 (s, 1H, OH), 8.14 (d, *J* = 9.2 Hz, 2H, Ar-H). ¹³C NMR (100 MHz, CDCl₃, δ, ppm): 13.83, 38.99, 40.14, 41.86, 51.94, 123.99, 128.41, 146.98, 150.62, 155.69, 171.86. LC-MS (*m/z*): 280.

Methyl-5-(hydroxyimino)-3-(2-nitrophenyl)hexanoate (**7h**): Color: White solid. Yield: 90%. M.p.: 82-84 °C. FT-IR (KBr, ν, cm⁻¹): 3210 (NH) and 1713 (C=O). ¹H NMR (400 MHz, DMSO-d_6, δ, ppm): 1.66 (s, 3H, CH₃), 2.68-2.77 (m, 4H, CH₂), 3.41 (s, 3H, OCH₃), 3.80 (t, *J* = 6.1 Hz, 1H, CH), 7.40 (d, *J* = 6.9 Hz, 1H, Ar-H), 7.60-7.76 (m, 3H, Ar-H), 10.37 (s, 1H, OH). ¹³C NMR (100 MHz, DMSO-d_6, δ, ppm): 14.06, 32.92, 41.50, 51.88, 124.23, 128.14, 129.31, 133.42, 137.88, 150.49, 153.41, 172.04. LC-MS (*m/z*): 280.

Methyl-5-(hydroxyimino)-3-(2-hydroxyphenyl)hexanoate (**7i**): Color: Brown solid. Yield: 85%. M.p.: 92-94 °C. FT-IR (KBr, ν, cm⁻¹): 3240 (NH) and 1710 (C=O). ¹H NMR (400 MHz, DMSO-d_6, δ, ppm): 1.90 (s, 3H, CH₃), 2.38 (m, 2H, CH₂), 2.46 (m, 2H, CH₂), 3.47 (s, 1H, CH), 3.68 (m, 3H, OCH₃), 7.76-7.39 (m, 4H, Ar-H), 8.02 (t, *J* = 8.0 Hz, 1H, OH). ¹³C NMR (100 MHz, DMSO-d_6, δ, ppm): 13.66, 30.92, 40.05, 51.38, 117.9, 125.10, 130.3, 132.41, 133.40, 157.38, 161.49, 172.14. LC-MS (*m/z*): 251.

Methyl-5-(hydroxyimino)-3-(2-hydroxynaphthalen-1-yl) hexanoate (**7j**): Color: Brown solid. M.p.: 96-98 °C. FT-IR (KBr, ν, cm⁻¹): 3200 (NH) and 1720 (C=O). ¹H NMR (400 MHz, DMSO-d_6, δ, ppm): 1.89 (s, 3H, CH₃), 2.64 (m, 2H, CH₂), 2.75 (m, 2H, CH₂), 3.68 (m, 1H, CH), 3.87 (s, 3H, OCH₃), 7.50 (d, *J* = 8.8 Hz, 2H, Ar-H), 7.82 (d, *J* = 7.8 Hz, 2H, Ar-H), 8.20 (t, *J* = 8.6 Hz, 2H, Ar-H), 9.85 (s, 1H, OH). ¹³C NMR (100 MHz, DMSO-d_6, δ, ppm): 15.04, 27.4, 37.6, 42.04, 51.10, 108.44, 119.46, 125.72,

126.54, 127.9, 130.40, 131.60, 134.50, 1593.12, 162.60, 172.9. LC-MS (*m/z*): 301.

Methyl-3-(3-bromophenyl)-5-(hydroxyimino)hexanoate (**7k**): Color: Light grey solid. Yield: 96%. M.p.: 86-88 °C. FT-IR (KBr, ν, cm⁻¹): 1740 and 1698. ¹H NMR (400 MHz, DMSO-d_6, δ, ppm): 2.1 (s, 3H, CH₃), 2.34-2.48 (m, 2H, CH₂), 2.52-2.70 (m, 2H, CH₂), 3.28 (m, *J* = 7.6 Hz, 1H, CH), 3.50 (s, 3H, OCH₃), 7.21 (m, *J* = 8.0 Hz, 1H, Ar-H), 7.38-7.52 (m, *J* = 8.1 Hz, 1H, Ar-H), 7.38 (m, *J* = 8.1, Hz, 1H, Ar-H), 7.52 (m, *J* = 7.4, Hz, 1H, Ar-H) 10.29 (s, 1H, OH). ¹³C NMR (100 MHz, DMSO-d_6, δ, ppm): 14.10, 39.16, 42.22, 51.96, 119.96, 128.84, 131.59, 131.95, 132.14, 143.39, 153.87, 172.35. LC-MS (*m/z*): 313.

Methyl-3-(4-bromophenyl)-5-(hydroxyimino)hexanoate (**7l**): Color: Grey. Yield: 90%. M.p.: 76-78 °C. FT-IR (KBr, ν, cm⁻¹): 3250 (-NH), 1726 (C=O). ¹H NMR (400 MHz, DMSO-d_6, δ, ppm): 1.62 (s, 3H, CH₃), 2.31-2.41 (m, 2H, CH₂), 2.52-2.70 (m, 2H, CH₂), 3.31 (s, 1H, CH), 3.44 (s, 3H, OCH₃), 7.17 (d, *J* = 8.4 Hz, 2H, Ar-H), 7.40 (d, *J* = 7.6 Hz, 2H, Ar-H), 10.28 (s, 1H, OH). ¹³C NMR (100 MHz, DMSO-d_6, δ, ppm): 13.96, 38.76, 41.98, 51.80, 119.96, 130.34, 131.59, 143.39, 153.74, 172.29.

2.3. Anti-inflammatory properties

The anti-inflammatory effect of the test compounds was assessed by the denaturation of bovine serum albumin, as described by Mizushima *et al.* and Sakat *et al.* [32,33]. The test samples were mixed with a 1% bovine albumin solution kept at pH = 6.4 with phosphate buffer saline. Furthermore, samples were incubated for 20 minutes at 37 °C, followed by 20 minutes at 57 °C. The absorbance was measured at 660 nm using a UV-Visible spectrophotometer after cooling (Eppendorf Bio spectrophotometer basic). The experiment was repeated three times with diclofenac sodium as the control medication. The percentage of inhibition of albumin denaturation was calculated using Equation (1).

$$\% \text{ Inhibition} = \frac{[\text{Absorbance control} - \text{Absorbance sample}] \times 100}{\text{Absorbance control}} \qquad (1)$$
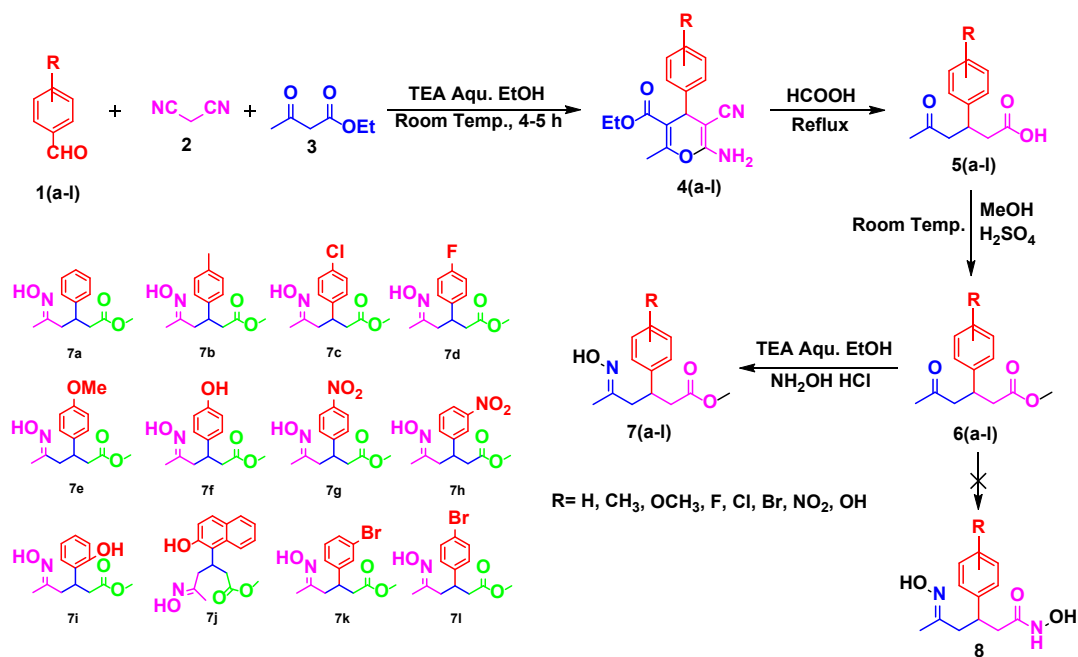
2.4. ABTS radical scavenging assay

The ABTS radical was created by reacting 7 mmol ABTS in H₂O with 2.45 mmol potassium persulphate and stored it at room temperature for 24 hours in the dark [34]. The ABTS solution was diluted with milli Q water before use to achieve an absorbance of 0.700-0.025 at 734 nm. The test chemical solutions with different concentrations (20, 40, 60, 80, and 100 µg/mL) were then given 1 mL of ABTS solution. Each concent-ration's % inhibition was measured at 734 nm after 6 minutes. The following equation was used to compute the scavenging ability of the ABTS radical:

$$\text{ABTS radical scavenging ability (\% I)} = [A_c - A_s / A_c] \times 100 \qquad (2)$$

where, A_c = Absorbance of control and A_s = Absorbance of sample

2.5. DPPH radical scavenging assay

The DPPH assay was used to determine the free radical scavenging activity of the test compounds [35]. In separate test tubes, a 100 µL solution of test samples from various concent-ration ranges (20, 40, 60, 80, and 100 µg) was added, followed by a 900 µL (0.1 mM) ethanolic DPPH solution. All test solutions, as well as the standard (ascorbic acid), were stored in a dark incubator at 37 °C for 30 minutes. A UV-Visible spectrophoto-meter was used to measure the absorbance at 517 nm. To get the mean standard deviation data, the test was conducted in three separate sets. An equation was used to compute the percent inhibition of the DPPH test.

Scheme 3. Synthesis of methyl-5-(hydroxyimino)-3-(aryl-substituted)hexanoate derivatives, **7a-l**.

DPPH radical scavenging ability (% I) = [A_c − A_s / A_c] × 100   (3)

where, Ac = Absorbance of control and As = Absorbance of sample. When the DPPH is scavenged by an antioxidant its absorbance gets decreased considerably.

2.6. In vitro antibacterial activity

The agar well diffusion technique was used to test the antibacterial activity of the produced compounds **7a-l** against Gram-positive bacteria *Staphylococcus aureus* (NCTC 10788), *Bacillus Subtilis* (NCIM2063), and Gram-negative *Escherichia coli*. Swab inoculated 100 µL of the test organisms onto sterile nutrient agar plates. A sterile cork borer was used to drill the wells into the agar plates [34]. In the matching wells, test compounds with concentrations of 600 and 1200 µg/mL were introduced. The plates were incubated at 37 °C for 24 hours, after which the zones of inhibition were seen and measured in millimeters.

2.7. Molecular docking

For the docking investigation, the Protein Data Bank was used to get the crystal structure of *E. coli* DNA gyrase B's 24 kDa domain in association with a small molecule inhibitor (PDB ID: 4DUH, X-Ray Diffraction, 1.50). Water molecules were removed from the proteins and polar hydrogen atoms with Gasteiger-Huckel charges were added to prepare them for docking. The ligands' 3D structures were generated using the SKETCH module of the SYBYL curriculum (Tripos Inc., St. Louis, USA), and their energy-minimized conformations were obtained using the Tripos force field with Gasteiger-Huckel [36] charges. Molecular docking was performed using the Surflex Dock program, which is interfaced with Sybyl-X 2.0 [37] and the software's configurations were assigned to a variety of additional parameters.

2.8. Cytotoxic activity

In the present study, the cytotoxic activity of synthesized organic compounds were tested on the lung cancer cells (A549)

by following the MTT [2-(4,5-dimethylthiazol-2-yl)-3,5-diphenyl-2*H*-tetrazol-3-ium bromide] assay [38]. According to the protocol required cell culture count was adjusted to 1.0×10^5 cells/mL using Dulbecco's Modified Eagle Medium (DMEM) which is supplemented with 10% FBS and seeded to 96-well microtiter plates (Falcon, Becton-Dickinson, Franklin Lakes, NJ, USA). After 24 hrs.; of plating, cells were serum starved for 24 hrs. After the proper growth was achieved, different concentrations of test samples were added to the culture media in 96 well plate and incubated for 24 hrs. After incubation medium was removed and 200 µL of DMSO was added and the amount of formazan formed was measured at 595 nm on a Model 680 Microplate reader (Bio-Rad Laboratories, Inc., Hercules, CA, USA). The percentage growth inhibition was calculated using the following formula and the concentration of test drugs needed to inhibit cell growth by 50% (IC$_{50}$) were generated from the dose-response curves for each cell line. This assay is based on the reduction of MTT by the mitochondrial dehydrogenase of intact cells to a purple formazan product [39-41].

Inhibition percentage = OD of test sample ÷ OD of control × 100   (4)

3. Results and discussion

3.1. Chemistry

The current research focuses on the synthesis of methyl-5-(hydroxyimino)-3-(aryl-substituted)hexanoate derivatives (**7a-l**), which is outlined in Scheme 3. The required substituted pyrans (**4a-l**) were originally synthesized using a one-pot multicomponent green approach [30]. Heating of compounds **4a-l** in formic acid gave compounds **5a-l** [31]. In the presence of a catalytic amount of sulphuric acid, the esterification products **6a-l** were produced. Furthermore, we anticipated isolating hydroxamic acid of ketoximes (**8a-l**) from compounds **6a-l** by over-reacting with hydroxylamine. The spectral data did not support the predicted outcome products **8a-l**. At ambient temperature and even under reflux conditions, the chemo selective products **7a-l** were formed; the spectral data such as IR, NMR, and mass hold the structures **7a-l** instead of compounds **8a-l**.

Table 1. Results of *in vitro* anti-inflammatory activity of the compounds **7a-l**.

Sample	% Inhibition of albumin denaturation					IC_{50}
	Concentration, μg/mL					
	20	40	60	80	100	
7a	0	2.431±0.12	5.83±0.28	9.72±0.47	15.55±0.75	214.51±6.24
7b	33.70±2.52	47.93±3.59	62.92±4.71	71.91±5.38	78.65±5.89	38.59±5.26
7c	74.74±7.15	77.61±7.42	87.19±8.33	91.95±7.41	93.88±6.36	7.17±0.48
7d	14.31±0.73	24.53±1.25	30.15±1.54	45.49±2.32	50.08±2.56	101.77±8.18
7e	34.95±6.37	46.45±6.91	71.89±9.21	84.23±7.92	93.27±6.7	34.90±7.34
7f	62.92±4.71	72.65±5.44	74.90±5.61	84.64±6.33	86.14±6.44	10.88±1.35
7g	35.20±2.63	48.75±2.15	64.47±2.49	74.22±2.93	88.46±3.74	37.97±4.92
7h	8.98±0.05	10.66±0.06	19.77±0.12	23.77±0.19	28.88±0.17	240.70±2.41
7i	80.15±5.99	83.89±6.28	86.14±6.44	87.64±6.56	95.65±4.84	2.61±0.15
7j	1.96±0.03	20.49±0.33	37.38±0.61	52.79±0.86	68.53±1.12	74.12±1.11
7k	10.73±0.55	20.95±1.07	32.70±1.67	50.59±2.58	67.97±3.47	76.92±3.81
7l	64.41±4.82	77.78±3.69	81.32±4.59	83.89±6.28	86.14±6.44	9.13±0.41
Diclofenac	42.49±4.07	57.16±2.8	75.45±3	83.05±2.83	93.76±2.98	27.43±3.04

* Results are expressed as mean±SD, n = 3. Correlation is significant at the 0.01 level.

Spectroscopic analysis of the formed products confirmed their structures. In the case of compound **7g**, the IR showed a stretching band at 3215 cm^{-1} indicating OH group of oxime and a stretching band of carbonyl group was observed at 1723 cm^{-1} indicating the presence of ester carbonyl but not the carbonyl of hydroxamic acid which was expected at lower frequency. In LC-MS, (M+1) peak was observed *m/z* 281, confirming the mass of compound **7g**. The ^1H NMR spectrum supports the formation of compound **7g**, wherein the methyl group of ketoximes appeared as a singlet at δ 1.82 ppm. The multiplet and doublet of doublet at δ 2.50 and 2.73 ppm due to methylene groups adjacent to the oxime group and to ester, respectively. Singlet at δ 3.57 ppm is due to methyl of ester and methine proton appeared as a quintet at δ 3.67 ppm. Phenyl protons appeared as a doublet at δ 7.35 (*J* = 8.4 Hz) and 8.14 ppm (*J* = 9.2 Hz), respectively. The ketoximes O-H appeared as a singlet at δ 8.02 ppm. In ^{13}C NMR spectrum of compound **7g** showed eleven distinct resonance signals. Carbonyl carbon resonated at δ 171 ppm; imine carbon showed a peak at δ 155 ppm, in addition four aromatic carbons resonated in the range of δ 123-150 ppm. Methyl carbon of ester showed a peak at δ 51 ppm, methylene carbons in the vicinity of imine and carbonyl resonated at δ 41 and 40 ppm, C_3 carbon showed a peak at δ 38 ppm and even structure elucidation is supported by DEPT-135 analysis to confirm odd and even proton containing carbons whose values are well in agreement with proposed oxime structure.

3.2. Pharmacological screening

The successfully synthesized molecules **7a-l** were screened for their anti-inflammatory, antibacterial, and antioxidant activities.

3.2.1. In vitro anti-inflammatory activity

From Table 1, the anti-inflammatory activity results of the compounds were very impressive with low half maximal at micro molar concentration, which was found to be better than the standard drug, diclofenac. Presence of electron donating hydroxy groups at para (**7f**) and ortho (**7i**) position on phenyl ring showed significant activity with IC_{50} = 10.88 and 2.61 as compared with standard diclofenac IC_{50} = 27.43, while the hydroxy group at C_2 position of naphthalene (**7i**) ring has showed drastically decrease in the activity. Replacing the hydroxy group by methoxy (**7e**) at para position of the phenyl ring showed two-fold less potent. The halogen substituted compounds such as chloro, bromo, and fluoro on phenyl ring were screened, wherein chloro (**7c**) and bromo (**7l**) substituted at para position and found to be more active with IC_{50} = 7.17 and 9.13, respectively. Whereas fluoro (**7d**) substitutions at para and bromo (**7k**) at meta position are not showing enhancement in their activity. The strong electron withdrawing group such as nitro group exhibited varying in their anti-inflammatory activity. Nitro group at para position (**7g**) on phenyl ring showed significantly good than the nitro group substituted at meta position (**7h**), compound **7b** having methyl group at para position exhibited good anti-inflammatory activity with IC_{50} = 38.59 and without substitution on phenyl ring (**7a**) found to be moderate activity. From the anti-inflammatory results, we can conclude that the electron donating groups on the phenyl ring at ortho and para position are exceptionally good than the meta position and without substitution.

3.2.2. In vitro antioxidant activity

To understand the vital role of the target oximes with different substitution at phenyl ring on different position towards antioxidant properties. All synthesized targets were subjected to *in vitro* antioxidant assay using 2,2'-azino-bis(3-ethylbenzthiazoline-6-sulphonic acid (ABTS) radical scavenging and 2,2-diphenyl-1-picrylhydrazyl (DPPH) radical scavenging activity [34,35].

3.2.2.1. ABTS radical scavenging assay

The synthesized oxime molecules **7a-l**, with different concentrations (20, 40, 60, 80, and 100 μg/mL) were studied. The ABTS assay is the simplest and effective method to exploit antioxidant activity of the newly synthesized compounds. The method is based on the direct generation of blue/green ABTS radical chromophores through the reaction between ABTS and potassium sulphate. From the antioxidant outcomes, the 50% inhibitory concentrations (IC_{50}) were calculated and are summarized in Table 2, the results indicate that the majority of compounds exhibited less scavenging ability. The incorporation of 2-naphtol on core (**7i**) showed better antioxidant activity compared to the other substitutions.

3.2.2.2. DPPH radical scavenging activity

The synthesized target compounds **7a-l** can quench DPPH free radicals and turn them to colorless (bleached product) i.e. [2,2-diphenyl-1-picrylhydrazyl hydrazine or substituted analogous hydrazine via transfer of hydrogen atoms or by electron donation by free radical attack on the DPPH molecule] leads to a decrease in absorbance. Therefore, the more rapidly the decrease in the absorbance, the more potent the radical scavenging activity of the compound [42]. The IC_{50} values of the compounds were determined and depicted in Table 3. The synthesized targets have less ability towards radical scavenging activity as compared to standard ascorbic acid, indicating that synthesized oximes are not potent antioxidant agents.

Table 2. *In vitro* antioxidant activity of compounds **7a-l** using ABTS method *.

Sample	ABTS radical scavenging ability					IC$_{50}$
	Concentration, µg/mL					
	20	40	60	80	100	
7a	5.19±0.07	6.65±0.09	8.92±0.10	11.04±0.15	13.15±0.18	464.19±6.83
7b	8.01±0.80	10.81±0.10	13.19±0.10	15.26±0.20	17.48±0.23	378.18±26.61
7c	1.29±0.01	1.62±0.02	3.57±0.04	4.87±0.06	6.00±0.08	784.85±10.69
7d	1.94±0.02	2.49±0.40	3.08±0.04	3.73±0.05	4.22±0.05	1684.41±89.20
7e	3.73±0.05	7.307±0.10	9.74±0.13	12.07±0.16	14.61±0.20	365.44±5.28
7f	3.49±0.04	6.20±0.08	8.90±0.10	11.60±0.10	14.30±0.19	364.16±5.07
7g	0.649±0.00	1.46±0.02	2.11±0.02	2.59±0.03	3.41±0.04	1500.27±20.73
7h	0.64±0.00	1.94±0.02	2.11±0.02	2.59±0.03	4.3836±0.06	1227.23±19.81
7i	1.74±0.02	5.40±0.07	9.06±0.12	12.71±0.17	16.37±0.22	263.07±3.76
7j	3.84±0.09	13.80±0.10	25.97±0.50	36.69±0.50	43.99±0.60	85.08±1.22
7k	4.81±0.60	6.27±0.50	7.89±0.57	9.68±0.50	11.46±0.50	562.10±4.83
7l	2.06±0.02	3.33±0.04	7.15±0.09	8.26±0.11	9.54±0.12	501.99±6.65
Standard (Ascorbic acid)	38.4±1.20	53.25±1.00	74.79±1.10	89.83±1.10	97.96±1.10	33.189±1.47

* Results are expressed as mean±SD, n = 3, Correlation is significant at the 0.01 level.

Table 3. Results of *in vitro* antioxidant activity of the compounds **7a-l**.

Sample	DPPH radical scavenging ability					IC$_{50}$
	Concentration, µg/mL					
	20	40	60	80	100	
7a	7.723±0.03	9.02±0.03	10.33±0.043	11.63±0.049	12.78±0.26	683.53±24.69
7b	5.91±0.05	7.80±1.24	8.64±0.07	10.46±0.09	10.92±0.10	680.02±13.53
7c	3.08±0.02	3.8±0.03	5.09±0.04	6.20±0.02	7.36±0.10	879.21±11.52
7d	4.09±0.03	4.29±0.03	4.49±0.03	4.69±0.04	4.89±0.03	4781.24±0.78
7e	13.53±0.12	14.55±0.13	15.80±0.14	15.80±0.14	18.42±0.17	621.02±7.48
7f	5.29±0.04	7.19±0.05	8.68±0.07	10.98±0.08	12.98±0.10	487.24±4.12
7g	0.22±0.002	0.787±0.005	1.43±0.03	1.54±0.44	2.67±0.02	1757.66±143.97
7h	4.59±0.03	5.09±0.04	5.69±0.04	6.19±0.05	6.79±0.05	1673.91±16.43
7i	8.52±0.07	11.03±0.10	13.87±0.12	16.37±0.14	19.71±0.42	321.48±6.73
7j	15.58±0.14	18.53±0.16	21.83±0.20	23.77±0.21	26.38±0.24	274.33±3.57
7k	4.46±0.51	5.66±0.51	6.67±0.51	7.75±0.56	9.50±0.51	769.16±10.76
7l	10.80±0.09	12.05±0.48	13.87±0.12	14.67±0.13	15.23±0.13	699.16±15.19
Standard (Ascorbic acid)	35.9±0.69	67.75±0.86	72.43±1.59	91.88±0.99	95.80±1.02	28.38±1.01

* Results are expressed as mean±SD, n = 3, Correlation is significant at the 0.01 level.

Table 4. Results of *in vitro* antibacterial activity of the compounds **7a-l**.

Sample	Zone of inhibition (mm)					
	S. aureus		*B. subtilis*		*E. coli*	
	600 µg/mL	1200 µg/mL	600 µg/mL	1200 µg/mL	600 µg/mL	1200 µg/mL
7a	-	12.33	-	8.67	-	-
7b	8.4	21	8.0	19	-	9.7
7c	11.5	15.67	11.83	15.67	-	8.33
7d	8.5	21.67	5.5	17.83	-	-
7e	-	-	-	-	-	-
7f	-	9.67	-	9	-	-
7g	-	-	-	-	-	-
7h	-	-	-	-	-	-
7i	11	27	9	22.67	-	-
7j	5.4	15.17	4.5	12.17	-	10.67
7k	9	23	-	10.67	-	8.33
7l	-	8.7	-	8.2	-	4.9
Streptomycin	22.66	24.5	18.58	20.67	25.5	28.33

The 50% inhibitory concentration (IC$_{50}$) profile of both methods (i.e., ABTS and DPPH) is compared with standard and synthesized compounds, which are supplied in Table 3.

3.3. In vitro antibacterial activity

All synthesized oxime derivatives were examined for their *in vitro* antibacterial activity against *Staphylococcus aureus*, *Bacillus subtilis*, and *Escherichia coli* by agar well diffusion method with Streptomycin as a standard. From Table 4, the antibacterial activity results revealed that some of the compounds exhibit good zone of inhibition against tested microorganisms. Compound **7b** methyl group at *para* position of phenyl ring was found to be half of the inhibition at low concentration (600 µg/mL) as compared with standard *Streptomycin*. In the case of *E. coli*, compounds **7b**, **7c**, **7j**, **7k**, and **7l** have shown moderate activity at 1200 µg/mL. Compound **7i** with hydroxy substituent at the ortho position of phenyl ring shown excellent activity compared to standard streptomycin at 1200 µg/mL. Introduction of methoxy (**7e**), hydroxy (**7f**), nitro (**7g**) on phenyl ring at *para* position and

nitro at *meta* position failed to show the inhibition antibacterial activity at both concentration against both Gram positive and Gram negative bacteria and 2-napthanol derivative (**7j**) demonstrated moderate activity against tested microorganism.

3.4. In vitro cytotoxic activity

The cytotoxic activity study was performed at different concentrations (10, 20, 30, 40, and 50 µg/mL) against lung cancer cell line (A549) by *in vitro* MTT cell viability assay. In present study, untreated A549 cells were considered as control group, whereas cis-platin treated A549 cells were considered as positive control. The results showed that, in comparison with the control group, the tested group cells showed decreasing in the cell viability with an increase in the concentration. In treated group there are many changes have observed with the morphological features of the cells, which were detached from the media and there is lysis and decrease in the cells count seen with some apoptotic features like cell breakage, cell shrinkage and apoptotic bodies, whereas normal cells appeared as regular and firm in shape [43-45].

Table 5. IC$_{50}$ value of test compounds against lung cancer A549 cells.

Sample	IC$_{50}$ in µg
7a	30.11
7b	29.90
7c	49.51
7d	18.91
7e	40.13
7f	59.50
7g	44.72
7h	46.90
7i	38.60
7j	56.93
7k	40.81
7l	29.80
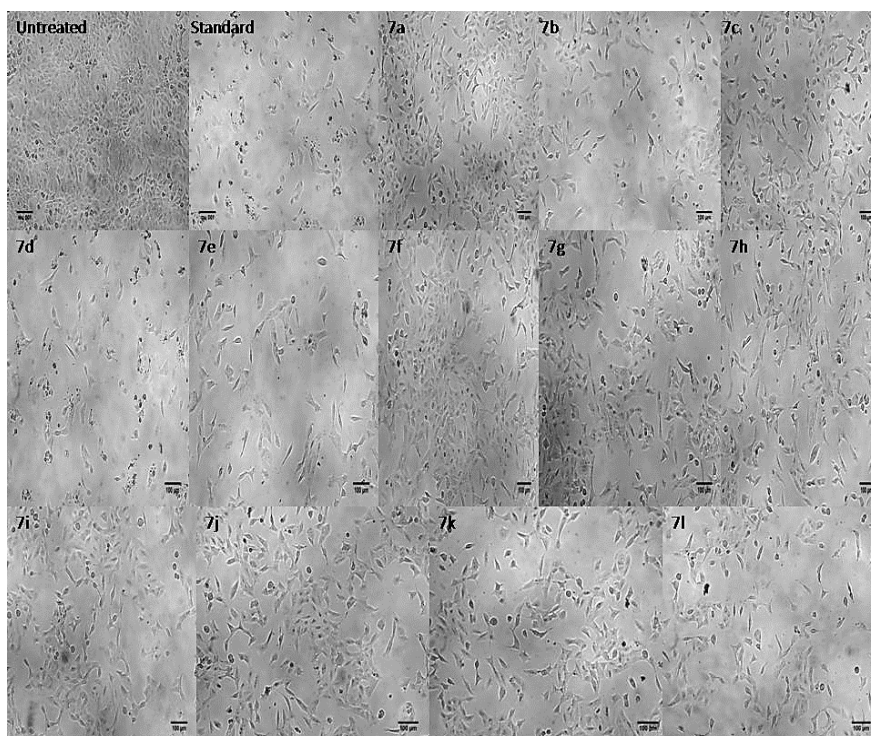
Figure 1. Morphological study of test samples against lung cancer A549 cells.

Microscopic examination revealed that morphological changes and shrinkage of cells occurred, leading to cell apoptosis induced by the tested compounds (Figure 1). Among the tested samples, the compound **7d** had shown the lowest IC$_{50}$ value and proven to be significant activity. The results are shown in Table 5.

3.5. Molecular docking studies

To examine the binding interaction of the synthesized molecules for antibacterial activity, some of the molecules were docked against *E. coli* DNA gyrase B in complex with a small molecule inhibitor (PDB ID: 4DUH, X-Ray Diffraction, 1.50 Å). The docking study revealed that all compounds have showed very good docking score against *E. coli.* (Figure 2) represents the docked view of all synthesized compounds at the active site of the enzyme PDB ID 4DUH.

As depicted in Figure 3, compound **7g** makes eight hydrogen bonding interactions at the active site of the enzyme (PDB ID: 4DUH), among them two interactions raised from oxygen atom of nitro group present at the 4th position of phenyl ring with hydrogen atoms of ARG136 (O···H-ARG136; 2.04 Å, 2.06 Å), nitrogen atom of nitro group present at the 4th position of phenyl ring makes a hydrogen bonding interaction with hydrogen atom of ARG136 (N···H-ARG136; 2.75 Å), hydrogen

atom of hydroxy group present at 5th position of hexanoate makes hydrogen bonding interactions with oxygen atoms of ASP49 and ASN46 (H···O-ASP49, 2.25 Å; H···O-ASN46, 1.86 Å), nitrogen atom imino group makes hydrogen bonding interactions with hydrogen atoms of ASN46 and LYS103 (N···H-ASN46, 2.85 Å; N···H-LYS103, 2.25 Å), and remaining hydrogen bonding interaction raised from the oxygen atom of hydroxy group present at 5th position of hexanoate with hydrogen of ASN46 (O···H-ASN46; 1.91 Å).

As depicted in Figure 4, compound **7e** makes seven hydrogen bonding interactions at the active site of the enzyme (PDB ID: 4DUH), among them three interactions raised from hydrogen atom of hydroxy group present at 5th position of hexanoate with oxygen atoms of THR165 and ASP73 (H···O-THR165,2.51 Å; H···O-ASP73,2.47 Å, 2.21 Å), oxygen atom of hydroxy group present at 5th position of hexanoate makes hydrogen bonding interactions with hydrogen atoms of THR165 and GLY77 (O···H-THR165, 2.16 Å; O···H-GLY77, 1.95 Å), and remaining two hydrogen bonding interactions raised from the nitrogen atom of imino group with hydrogen atoms of THR165 and GLY77 (N···H-THR165, 1.88 Å; N···H-GLY77, 2.82 Å). As depicted in Figure 5, 4DUH_Ligand makes six hydrogen bonding interactions at the active site of the enzyme (PDB ID: 4DUH). Figure 6 represents the hydrophobic and hydrophilic amino acids surrounded to the studied compounds **7g** and **7e.**

Table 6. Surflex docking score (kcal/mol) of the derivatives for *E. coli* (PDB ID: 4DUH).

Sample	C Score [a]	Crash Score [b]	Polar Score [c]	D Score [d]	PMF Score [e]	G Score [f]	Chem Score [g]
4DUH Ligand	10.33	-0.74	5.44	-153.236	-71.499	-304.003	-39.479
7g	8.95	-1.47	4.80	-113.495	-58.699	-207.371	-26.112
7e	7.93	-2.06	2.66	-129.268	-18.554	-259.957	-25.568
7b	7.89	-2.27	2.32	-118.613	-8.305	-260.269	-24.033
7f	7.61	-1.56	3.54	-112.149	-23.508	-215.522	-22.180
7i	7.48	-1.92	3.37	-120.136	-18.238	-234.898	-23.955
7d	7.32	-1.75	2.71	-116.689	-8.326	-242.256	-23.700
7a	6.66	-2.53	3.46	-115.881	-29.880	-210.087	-22.861
7j	6.59	-2.67	2.69	-129.332	-35.646	-265.661	-24.966
7c	6.18	-1.89	1.90	-119.973	-17.291	-217.152	-20.538
7h	5.31	-2.65	2.24	-114.636	-27.205	-245.253	-19.037

[a] C Score (Consensus Score) integrates several popular scoring functions for ranking the affinity of ligands bound to the active site of a receptor and reports the output of total score.
[b] Crash-score revealing the inappropriate penetration into the binding site. Crash scores close to 0 are favourable. Negative numbers indicate penetration.
[c] Polar indicates the contribution of the polar interactions to the total score. The polar score may be useful for excluding docking results that make no hydrogen bonds.
[d] D-score for charge and van der Waals interactions between the protein and the ligand.
[e] PMF-score indicating the Helmholtz free energies of interactions for protein-ligand atom pairs (Potential of Mean Force, PMF).
[f] G-score showing hydrogen bonding, complex (ligand-protein), and internal (ligand-ligand) energies.
[g] Chem-score points for H-bonding, lipophilic contact, and rotational entropy, along with an intercept term.
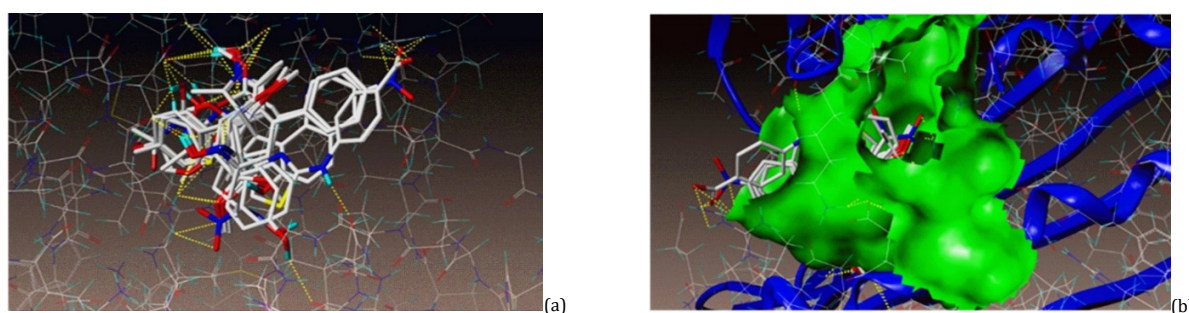

(a)

(b)

Figure 2. Docked view of all compounds at the active site of the enzyme PDB ID: 4DUH. (a) 3D view of compounds docked and (b) Docked view of compounds at the active site of enzyme.
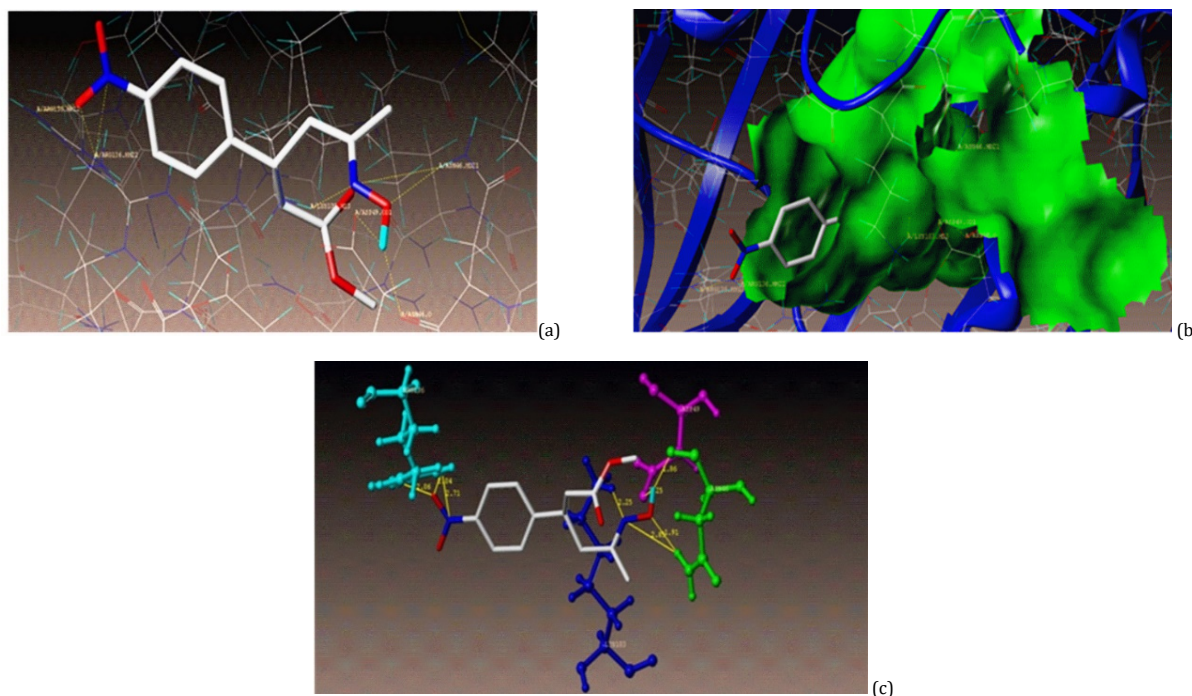

(a)

(b)

(c)

Figure 3. Docked view of compound **7g** at the active site of the enzyme PDB: 4DUH. (a) 3D view of compound **7g**, (b) Docked view of compound **7g** at the active pocket of enzyme, and (c) 2D view of compound **7g**.

All compounds showed consensus score in the range 8.95-5.31, indicating the summary of all forces of interaction between ligands and the enzyme. In addition, we saw that the studied compounds showed same type of interactions with amino acid residues (ARG136 and THR165) as that of reference 4DUH ligand. These scores indicate that molecules preferentially bind to DNA gyrase enzymes in comparison to the reference 4DUH ligand, Table 6.
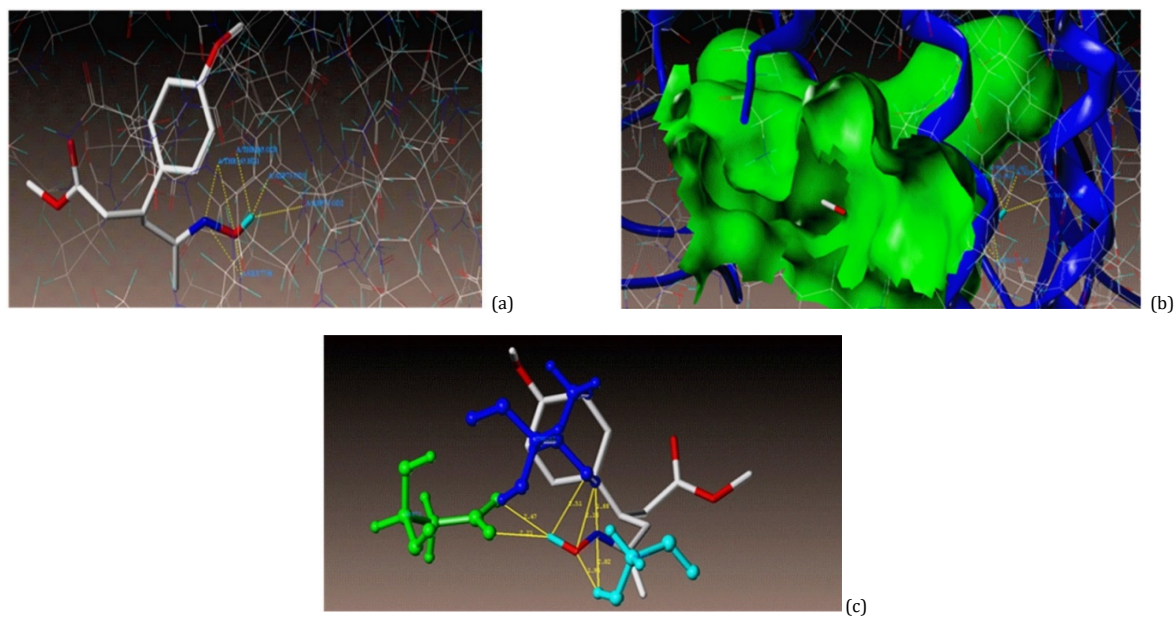
Figure 4. Interaction of compound **7e** at the binding site of the enzyme (PDB ID: 4DUH). (a) 3D view of compound 7e (b) Docked view of compound 7e at the active pocket of enzyme and (c) 2D view of compound **7e**.
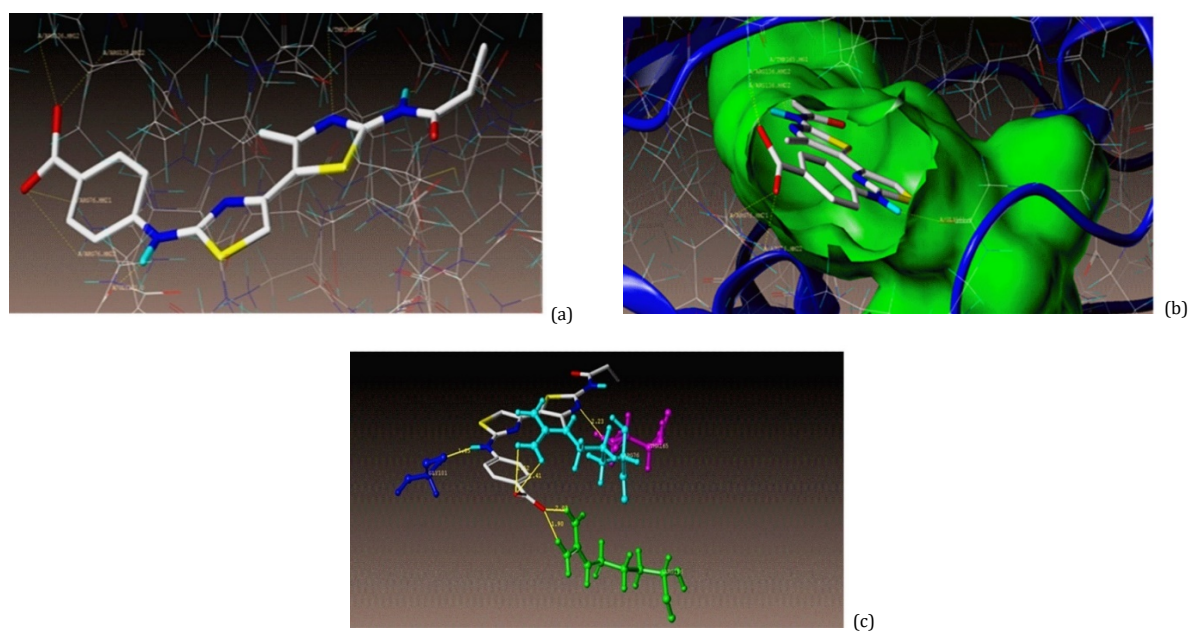

Figure 5. Docked view of 4DUH_Ligand at the binding site of the enzyme PDB ID: 4DUH. (a) 3D view of 4DUH_Ligand, (b) Docked view of 4DUH_Ligand at the active pocket of enzyme and (c) 2D view of 4DUH_Ligand.
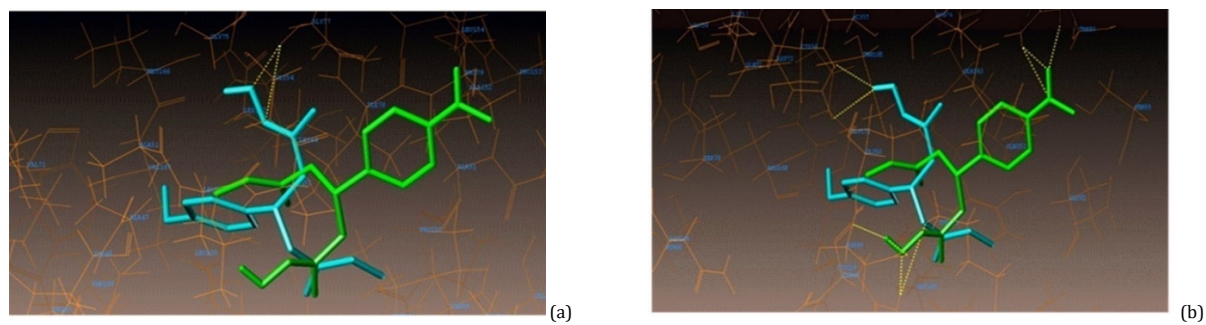

Figure 6. (a) Hydrophobic amino acids surrounded to compounds **7g** (green colour) and **7e** (cyan colour). (b) Hydrophilic amino acids surrounded to compounds **7g** and **7e**.

4. Conclusion

In summary, using a simple experimental approach and a short reaction time we synthesized a series of new methyl-5-(hydroxyimino)-3-(aryl-substituded)hexanoate oxime derivatives **7a-l** using triethylamine as a catalyst under conventional reaction conditions in high yield. The anti-inflammatory, antioxidant, and antibacterial properties of the products were investigated. Compounds **7c**, **7f**, **7i**, and **7l** were discovered to have strong anti-inflammatory action. Majority of the compounds have modest antioxidant activity when examined using ABTS and DPPH free radical scavenging techniques. In terms of antibacterial activity against a specific bacterial strain, compound **7i** showed promising activity in both concentrations against Gram-positive bacteria, whereas other compounds only showed activity at higher concentrations (1200 g/mL), and compounds **7b**, **7c**, **7j**, **7k**, and **7l** showed moderate activity only against *E. coli*. The cytotoxic activity study showed that the compounds have significant activity against lung cancer cell line.

Acknowledgements

Disclosure statement DS

Conflict of interest: The authors declare that they have no conflict of interest.
Ethical approval: All ethical guidelines have been adhered.
Sample availability: Samples of the compounds are available from the author.

CRediT authorship contribution statement CR

Conceptualization: Parashuram Gudimani, Lokesh Anand Shastri; Methodology: Parashuram Gudimani; Software: Shrinivas Joshi, Parashuram Gudimani; Validation: Parashuram Gudimani, Varsha Pawar; Formal Analysis: Parashuram Gudimani; Investigation: Shyamkumar Vootla, Sheela Khanapure; Data Curation: Parashuram Gudimani, Nagashree Uday Hebbar; Writing - Original Draft: Parashuram Gudimani, Nagashree Uday Hebbar; Writing - Review and Editing: Samundeeswari Lokesh Shastri, Vinay Sungar; Visualization: Parashuram Gudimani, Lokesh Anand Shastri; Supervision: Lokesh Anand. Shastri.

ORCID ID and Email ✉

Parashuram Gudimani
✉ rnpstkga@gmail.com
https://orcid.org/0000-0002-3131-1958
Samundeeswari Lokesh Shastri
✉ sseswari14@gmail.com
https://orcid.org/0000-0003-1035-7081
Varsha Pawar
✉ varshapawar183@gmail.com
https://orcid.org/0000-0003-2096-9356
Nagashree Uday Hebbar
✉ hebbarnagashree@gmail.com
https://orcid.org/0000-0002-8647-2724
Lokesh Anand Shastri
✉ drlashastri@kud.ac.in
https://orcid.org/0000-0002-5672-8442
Shrinivas Joshi
✉ shrinivasdj@rediffmail.com
https://orcid.org/0000-0002-6520-806X
Shyam Kumar Vootla
✉ vootlashyam@gmail.com
https://orcid.org/0000-0002-7936-9825
Sheela Khanapure
✉ khanapuresheela@gmail.com
https://orcid.org/0000-0002-4247-1658

Vinay Sunagar
✉ vsunagar74@gmail.com
https://orcid.org/0000-0001-9804-7330

References

[1]. Nicolaou, K. C. Organic synthesis: the art and science of replicating the molecules of living nature and creating others like them in the laboratory. *Proc. Math. Phys. Eng. Sci.* **2014**, *470*, 20130690.
[2]. Mo, X.; Morgan, T. D. R.; Ang, H. T.; Hall, D. G. Scope and mechanism of a true organocatalytic Beckmann rearrangement with a boronic acid/perfluoropinacol system under ambient conditions. *J. Am. Chem. Soc.* **2018**, *140*, 5264–5271.
[3]. Koran, K.; Özen, F.; Biryan, F.; Görgülü, A. O. Synthesis, structural characterization and dielectric behavior of new oxime-cyclotriphosphazene derivatives. *J. Mol. Struct.* **2016**, *1105*, 135–141.
[4]. Xu, Y.; Yang, Q.; Li, Z.; Gao, L.; Zhang, D.; Wang, S.; Zhao, X.; Wang, Y. Ammoximation of cyclohexanone to cyclohexanone oxime using ammonium chloride as nitrogen source. *Chem. Eng. Sci.* **2016**, *152*, 717–723.
[5]. Sahyoun, T.; Arrault, A.; Schneider, R. Amidoximes and oximes: Synthesis, structure, and their key role as NO donors. *Molecules* **2019**, *24*, 2470.
[6]. Saikia, L.; Baruah, J. M.; Thakur, A. J. A rapid, convenient, solventless green approach for the synthesis of oximes using grindstone chemistry. *Org. Med. Chem. Lett.* **2011**, *1*, 12.
[7]. Karthikeyan, P.; Aswar, S. A.; Muskawar, P. N.; Sythana, S. K.; Bhagat, P. R.; Kumar, S. S.; Satvat, P. S. A novel l-amino acid ionic liquid for quick and highly efficient synthesis of oxime derivatives – An environmental benign approach. *Arab. J. Chem.* **2016**, *9*, S1036–S1039.
[8]. Walton, J. Functionalised oximes: Emergent precursors for carbon-, nitrogen- and oxygen-centred radicals. *Molecules* **2016**, *21*, 63.
[9]. Kozłowska, J.; Grela, E.; Baczyńska, D.; Grabowiecka, A.; Anioł, M. Novel O-alkyl derivatives of naringenin and their oximes with antimicrobial and anticancer activity. *Molecules* **2019**, *24*, 679.
[10]. Pal, D.; Kumar, S.; Saha, S. Antihyperglycemic activity of phenyl and ortho-hydroxy phenyl linked imidazolyl triazolo hydroxamic acid derivatives. *Int. J. Pharm. Pharm. Sci.* **2017**, *9*, 247–251.
[11]. Das, M.; Das, B.; Samanta, A. Antioxidant and anticancer activity of synthesized 4-amino-5-((aryl substituted)-4H-1,2,4-triazole-3-yl)thio-linked hydroxamic acid derivatives. *J. Pharm. Pharmacol.* **2019**, *71*, 1400–1411.
[12]. Pepeljnjak, S.; Zorc, B.; Butula, I. Antimicrobial activity of some hydroxamic acids. *Acta Pharm.* **2005**, *55*, 401–408.
[13]. Yousif, M. N. M. Recent advances in chemistry and biological activity of 2,6-diphenyl piperidines. *Mini Rev. Org. Chem.* **2022**, *19*, 125–135.
[14]. Dai, H.; Chen, J.; Li, H.; Dai, B.; He, H.; Fang, Y.; Shi, Y. Synthesis and bioactivities of novel pyrazole oxime derivatives containing a 5-trifluoromethylpyridyl moiety. *Molecules* **2016**, *21*, 276.
[15]. Kozłowska, J.; Potaniec, B.; Żarowska, B.; Anioł, M. Synthesis and biological activity of novel O-alkyl derivatives of naringenin and their oximes. *Molecules* **2017**, *22*.
[16]. Sammaiah, A.; Kaki, S. S.; Manoj, G. N. V. T. S.; Poornachandra, Y.; Kumar, C. G.; Prasad, R. B. N. Novel fatty acid esters of apocynin oxime exhibit antimicrobial and antioxidant activities: Novel bioactive lipophilic apocynin oxime esters. *Eur. J. Lipid Sci. Technol.* **2015**, *117*, 692–700.
[17]. Gopalakrishnan, M.; Thanusu, J.; Kanagarajan, V. A facile solid-state synthesis and in vitro antimicrobial activities of some 2,6-diarylpiperidin/tetrahydrothiopyran and tetrahydropyran-4-one oximes. *J. Enzyme Inhib. Med. Chem.* **2009**, *24*, 669–675.
[18]. Arthur-Santiago, M. A.; Oliart-Ros, R. M.; Sánchez-Otero, M. G.; Valerio-Alfaro, G. Mechanochemo-enzymatic Synthesis of Aromatic Aldehyde Oxime Ester. *Nat. Prod. Commun.* **2018**, *13*, 7, https://doi.org/10.1177/1934578X1801300723
[19]. Flipo, M.; Charton, J.; Hocine, A.; Dassonneville, S.; Deprez, B.; Deprez-Poulain, R. Hydroxamates: relationships between structure and plasma stability. *J. Med. Chem.* **2009**, *52*, 6790–6802.
[20]. Giacomelli, G.; Porcheddu, A.; Salaris, M. Simple one-flask method for the preparation of hydroxamic acids. *Org. Lett.* **2003**, *5*, 2715–2717.
[21]. Jamal, S. A. A.; Jaser, B.; Hmadi, W. F.; Al-Obaidi, O. Preparation Some of Hydroxamic Acid Derivatives from Honey Wax Compounds and Study the Biological Activity on Cancerous Tumors. *Sys. Rev. Pharm.* **2020**, *11* (2), 109–118.
[22]. Botta, C. B.; Cabri, W.; Cini, E.; De Cesare, L.; Fattorusso, C.; Giannini, G.; Persico, M.; Petrella, A.; Rondinelli, F.; Rodriquez, M.; Russo, A.; Taddei, M. Oxime amides as a novel zinc binding group in histone deacetylase inhibitors: synthesis, biological activity, and computational evaluation. *J. Med. Chem.* **2011**, *54*, 2165–2182.
[23]. Tharini, K.; Sangeetha, P. Antioxidant and anti-inflammatory activity of 3,3-dimethyl 2,6-dimethyl piperidine 4-one oxime. *Int. J. Chem. Sci.* **2015**, *13*, 1794–1804. https://www.tsijournals.com/articles/anti

oxidant-and-antiinflammatory-activity-of-33dimethyl-26dimethyl-piperidine-4one-oxime.pdf (accessed April 10, 2022).

[24]. El-Gamal, M. I.; Bayomi, S. M.; El-Ashry, S. M.; Said, S. A.; Abdel-Aziz, A. A.-M.; Abdel-Aziz, N. I. Synthesis and anti-inflammatory activity of novel (substituted)benzylidene acetone oxime ether derivatives: molecular modeling study. *Eur. J. Med. Chem.* **2010**, *45*, 1403–1414.

[25]. Naik, N. S.; Shastri, L. A.; Joshi, S. D.; Dixit, S. R.; Chougala, B. M.; Samundeeswari, S.; Holiyachi, M.; Shaikh, F.; Madar, J.; Kulkarni, R.; Sunagar, V. 3,4-Dihydropyrimidinone-coumarin analogues as a new class of selective agent against S. aureus: Synthesis, biological evaluation and molecular modelling study. *Bioorg. Med. Chem.* **2017**, *25*, 1413–1422.

[26]. Mallesha, L.; Mohana, K. Synthesis and In Vitro Antimicrobial Activity of 2,4-Difluorophenyl (piperidin-4-yl)methanone Oxime Derivatives. *Can. Chem. Trans.* **2014**, 343–352.

[27]. Jebli, N.; Hamimed, S.; Van Hecke, K.; Cavalier, J.-F.; Touil, S. Synthesis, antimicrobial activity and molecular docking study of novel α-(diphenylphosphoryl)- and α-(diphenylphosphorothioyl)cycloal-kaneone oximes. *Chem. Biodivers.* **2020**, *17*, e2000217.

[28]. Burcu, B.; Karaosmanoglu, O.; Dal, H.; Sivas, H.; Benkli, K. Synthesis of Some Aryl Ketoxime Derivatives with their in vitro Anti-microbial and Cytotoxic Activity. *Glob. J. Cancer. Ther.* **2019**, *5* (1), 001–006.

[29]. Premalatha, B.; Bhakiaraj, D.; Elavarasan, S.; Chellakili, B.; Gopalakrishnan, M. Synthesis, spectral analysis, in vitro microbiological evaluation and antioxidant properties of 2,4-diaryl-3-azabicyclo[3.3.1]nonane-9-one-O-[2,4,6-tritertiarybutyl-cyclohexa-2,5-dienon-4-yl] oximes as a new class of antimicrobial and antioxidant agents. *J. Pharm. Res.* **2013**, *6*, 730–735.

[30]. Saxena, A.; Shastri, L.; Sunagar, V. Green approach for the synthesis of 4-coumarin-4H-pyrans from 4-formylcoumarins and their antibacterial study. *Synth. Commun.* **2017**, *47*, 1570–1576.

[31]. Gudimani, P.; Shastri, S. L.; Pawar, V.; Shastri, L. A.; Sungar, V. A. Indirect, catalyst free β-arylation of acyclic 1,5-dicarbonyl compounds via green method. *Chem. Data Coll.* **2021**, *33*, 100692.

[32]. Sakat, S.; Juvekar, A.; Gambhire, M. In-vitro antioxidant and anti-inflammatory activity of methanol extract of Oxalis corniculata Linn. *Int. J. Pharm. Pharm. Sci.* **2010**, *2*, 146–155.

[33]. Mizushima, Y.; Kobayashi, M. Interaction of anti-inflammatory drugs with serum proteins, especially with some biologically active proteins. *J. Pharm. Pharmacol.* **1968**, *20*, 169–173.

[34]. Harini, S. T.; Kumar, H. V.; Rangaswamy, J.; Naik, N. Synthesis, antioxidant and antimicrobial activity of novel vanillin derived piperidin-4-one oxime esters: preponderant role of the phenyl ester substituents on the piperidin-4-one oxime core. *Bioorg. Med. Chem. Lett.* **2012**, *22*, 7588–7592.

[35]. Re, R.; Pellegrini, N.; Proteggente, A.; Pannala, A.; Yang, M.; Rice-Evans, C. Antioxidant activity applying an improved ABTS radical cation decolorization assay. *Free Radic. Biol. Med.* **1999**, *26*, 1231–1237.

[36]. Gasteiger, J.; Marsili, M. Iterative partial equalization of orbital electronegativity—a rapid access to atomic charges. *Tetrahedron* **1980**, *36*, 3219–3228.

[37]. Zhong, H.; Huang, W.; He, G.; Peng, C.; Wu, F.; Ouyang, L. Molecular dynamics simulation of tryptophan hydroxylase-1: binding modes and free energy analysis to phenylalanine derivative inhibitors. *Int. J. Mol. Sci.* **2013**, *14*, 9947–9962.

[38]. Carmichael, J.; DeGraff, W. G.; Gazdar, A. F.; Minna, J. D.; Mitchell, J. B. Evaluation of a tetrazolium-based semiautomated colorimetric assay: assessment of chemosensitivity testing. *Cancer Res.* **1987**, *47*, 936–942.

[39]. Mosmann, T. Rapid colorimetric assay for cellular growth and survival: application to proliferation and cytotoxicity assays. *J. Immunol. Methods* **1983**, *65*, 55–63.

[40]. Alley, M. C.; Scudiero, D. A.; Monks, A.; Hursey, M. L.; Czerwinski, M. J.; Fine, D. L.; Abbott, B. J.; Mayo, J. G.; Shoemaker, R. H.; Boyd, M. R. Feasibility of drug screening with panels of human tumor cell lines using a microculture tetrazolium assay. *Cancer Res.* **1988**, *48*, 589–601.

[41]. Scudiero, D. A.; Shoemaker, R. H.; Paull, K. D.; Monks, A.; Tierney, S.; Nofziger, T. H.; Currens, M. J.; Seniff, D.; Boyd, M. R. Evaluation of a soluble tetrazolium/formazan assay for cell growth and drug sensitivity in culture using human and other tumor cell lines. *Cancer Res.* **1988**, *48*, 4827–4833.

[42]. Blois, M. S. Antioxidant determinations by the use of a stable free radical. *Nature* **1958**, *181*, 1199–1200.

[43]. Zhang, S.-L.; Xie, H.-X.; Zhu, J.; Li, H.; Zhang, X.-S.; Li, J.; Wang, W. Organocatalytic enantioselective β-functionalization of aldehydes by oxidation of enamines and their application in cascade reactions. *Nat. Commun.* **2011**, *2*, 211.

[44]. Xu, Y.; Yang, Q.; Li, Z.; Gao, L.; Zhang, D.; Wang, S.; Zhao, X.; Wang, Y. Ammoximation of cyclohexanone to cyclohexanone oxime using ammonium chloride as nitrogen source. *Chem. Eng. Sci.* **2016**, *152*, 717–723.

[45]. Alturiqi, A. S.; Alaghaz, A.-N. M. A.; Ammar, R. A.; Zayed, M. E. Synthesis, spectral characterization, and thermal and cytotoxicity studies of Cr(III), Ru(III), Mn(II), Co(II), Ni(II), Cu(II), and Zn(II) complexes of Schiff base derived from 5-hydroxymethylfuran-2-carbaldehyde. *J. Chem.* **2018**, *2018*, 1–17.

[46]. Jean, B. P.; Franklin, R. C.; Patricia, A. B.; George, M. E.; Janet, A. H.; Stephen, G. J.; James, S. L.; Brandi, L.; Linda, A. M.; David, P. M.; Mair, P.; Jana, M. S.; Maria, M. T.; John, D. T.; Melvin, P. W.; Barbara, L. Z. Clinical and Laboratory Standards Institute *Performance standards for antimicrobial disk susceptibility test twenty-fifth informational supplement*; Committee for Clinical Laboratory Standards: Wayne PA, 2015.

[47]. Kahlmeter, G. The 2014 Garrod Lecture: EUCAST – are we heading towards international agreement? *J. Antimicrob. Chemother.* **2015**, *70*, 2427–2439.